Available online at www.sciencedirect.com

SciVerse ScienceDirect

Procedia Engineering 36 (2012) 246 – 252

Procedia Engineering

www.elsevier.com/locate/procedia

IUMRS-ICA 2011

The Low Electrical Resistivity of the High-entropy Alloy Oxide Thin Films

Chun-Huei Tsau*, Ya-Chu Yang, Cheng-Che Lee, Lyu-Yi Wu, and Hou-Jun Huang

Graduate school of Nanomaterials, Chinese Culture University, Taipei, Taiwan, ROC.
** Corresponding author. Tel.:+886-2-28610511; fax: +886-2-28618287.*
E-mail address: chtsau@staff.pccu.edu.tw

Abstract

This paper reports the new compositions of oxide thin films with very low electrical resistivity. We have found that some of the high-entropy alloy oxide thin films which still had very low electrical resistivity. In this study, we deposited the thin films of Ti_xFeCoNi (x=0, 0.25, 0.5, 0.75 and 1), TiFeCoNiCu_x (x=1, 2 and 3), and Al_xCrFeCoNiCu (x=0.5 and 1) by PVD, all the targets were prepared by arc-melting under Ar atmosphere. The microstructures of the specimens were examined by SEM and TEM; the electrical resistivities of the specimens were measured by four-point probe equipment. Results indicated the microstructures of the as-deposited alloy thin films were amorphous. All of the thin films were oxidized and became to semiconductors after annealed by vacuum furnace, also their microstructures transformed to nanocrystalline FCC microstructures. The electrical resistivities of these high entropy alloy oxides were about 30 μΩ-cm for the Ti_xFeCoNi oxide thin films, about 100 μΩ-cm for the TiFeCoNiCu_3 oxide thin film and about 650 μΩ-cm for the $Al_{0.5}$CrFeCoNiCu oxide thin film. That is, we found the new compositions of oxides with very low electrical resistivity. This is the most important result of this study, and it could also be very important contribution to the electrical ceramics.

Keywords: High-entropy; oxide thin film; TiFeCoNi; resistivity

1. Introduction

The semiconductors usually have higher electrical resistivity than metals because they have different charge carriers. [1, 2] The charge carriers of metals are free electrons, and those of the semiconductors are free conduction electrons and electrical holes. But two well-known semiconductor oxides exhibit metallic resistivity at room temperature. One is ruthenium dioxide (RuO_2) whose lowest achievable resistivity is

1877-7058 © 2012 Published by Elsevier Ltd. Open access under CC BY-NC-ND license.
doi:10.1016/j.proeng.2012.03.037

approximately 35 μΩ-cm in bulk single crystal. [3] The other is tin-doped indium oxide (ITO) thin film; whose lowest resistivity is approximately 150 μΩ-cm. [4] ITO thin films are widely applied in electronic devices, which require high transparency in the visible light region and low resistivity.

In our previously study based on the concept of high-entropy alloy, [5-7] we found several metal oxide thin films which exhibited metallic resistivity at room temperature, such as the resistivity of TiFeCoNi alloy oxide thin films only had 35 μΩ-cm. [8] Moreover, the other $Ti_xFeCoNi$ oxide thin films have lower resistivity. However, the Cu element had negative effect on the resistivity of these alloy oxide thin films. These results could be very important in the field of electronic ceramics.

2. Experimental procedures

The alloy targets were prepared by arc melting using appropriate amounts of pure elements, the purity of all of which exceeded 99.9%. The compositions of the alloy targets were listed in Table 1. A DC physical vapor sputtering (PVD) was used to deposit the metallic films. It was performed at 100 W and the flow rate of Ar was 30 standard cubic centimeter per min (sccm). The base and working pressures were 5×10^{-5} and 2×10^{-3} torr, respectively. Some of the samples were annealed using a vacuum furnace with a mechanical pump, and some of the samples were vacuum sealed in quartz tubes and then annealed in an air furnace. The compositions of the films were determined using an electron probe x-ray microanalyzer (EPMA, JEOL JXA-8800). The microstructural evolutions of the alloys were monitored using scanning electron microscopy (SEM) and transmission electron microscopy (TEM). SEM observations were made using a JEOL JSM-6335 field emission scanning electron microscope operated at 15 kV. TEM observations were made using a JOEL JEM-2010 transmission electron microscope operated at 200 kV. The room-temperature electrical resistivity of all samples films were measured with a four-point probe (Napson Corporation Model TR-70).

Table 1. Compositions of the alloy targets.

Alloys	Weight %						
	Al	Ti	Cr	Fe	Co	Ni	Cu
$Al_{0.5}CrFeCoNiCu$	4.5		17.2	18.5	19.4	19.4	21.0
AlCrFeCoNiCu	8.5		16.5	17.7	18.7	18.5	20.1
FeCoNi				32.2	34.0	33.8	
$Ti_{0.25}FeCoNi$		6.5		30.1	31.7	31.7	
$Ti_{0.5}FeCoNi$		12.1		28.3	30.0	29.6	
$Ti_{0.75}FeCoNi$		17.2		26.7	28.1	28.0	
TiFeCoNi		21.7		25.2	26.6	26.5	
TiFeCoNiCu		16.8		19.6	20.7	20.6	22.3
$TiFeCoNiCu_2$		13.7		16.0	16.9	16.8	36.6
$TiFeCoNiCu_3$		11.6		13.6	14.3	14.3	46.2

3. Results and discussion

3.1. As-deposited microstructures

Figure 1(a) is a typical cross-section SEM micrograph of the as-deposited specimen which shows the Si substrate, SiO_2 layer and the alloy thin films with columnar structure. Figure 1(b) shows the plan view morphology of the as-deposited alloy thin film. There are two kinds of black lines on the thin film. The

narrow black lines were identified as amorphous grain boundaries. The wide black lines are the cracks along the grain boundaries. Figure 2(a) shows the bright field TEM image, and Fig. 2(b) is the corresponding diffraction pattern which proves the amorphous structure. Donovan and Heineman first observed these amorphous grain boundaries in an evaporated amorphous Ge thin film [9], and they suggested that the formation of a void network resulted in density-deficient boundaries that are intrinsic to amorphous films. Tsukimoto *et al.* further described the mechanism of formation of amorphous grain boundaries in TaN thin films, following a detailed analysis [10]. The wide black lines along the amorphous grain boundaries are cracks, which were caused by the release of stress during and after the deposition of the thin films. All of the as-deposited metal thin films had an amorphous structure in present study, and this was also confirmed by XRD diffraction.

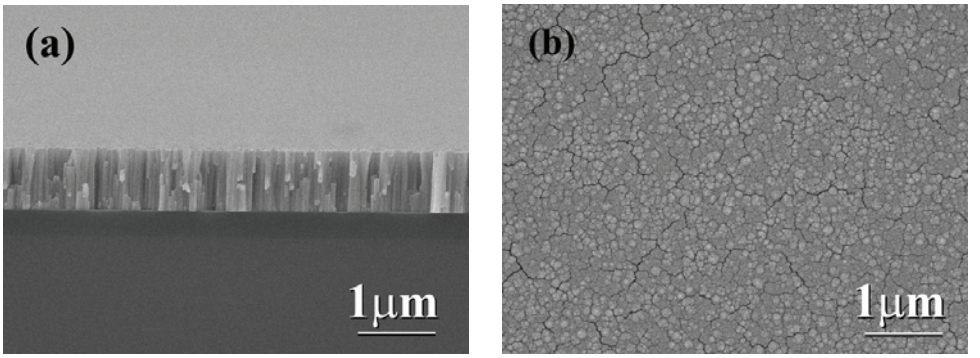

Fig. 1. SEM micrographs of as-deposited FeCoNi thin film, (a) cross section; and (b) plan view.

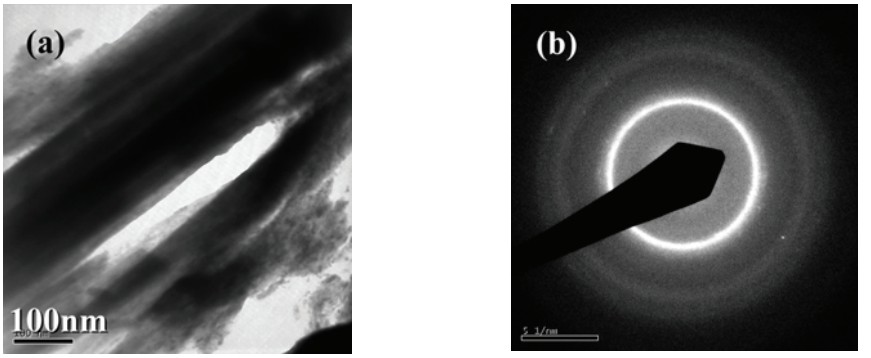

Fig. 2. TEM observation of FeCoNi alloy thin film, (a) bright field image; and (b) corresponding diffraction pattern.

3.2. As-annealed microstructures

Some of the thin films were annealed at various temperatures in a vacuum furnace. These films were indentified to be oxidized as metal oxide films by the small amount of oxygen in the chamber. Figure 3(a) and 3(b) show cross-section and plan-view micrographs of the $TiFeCoNiO_y$ oxide film after annealed at high temperature for a period. The thin films lost their columnar structure, the roughness of their surfaces increased and some alloy oxide precipitated on the surfaces. The amorphous grain boundaries are almost

invisible, indicating that annealing treatment can eliminate small voids at amorphous grain boundaries through the oxidizing process.

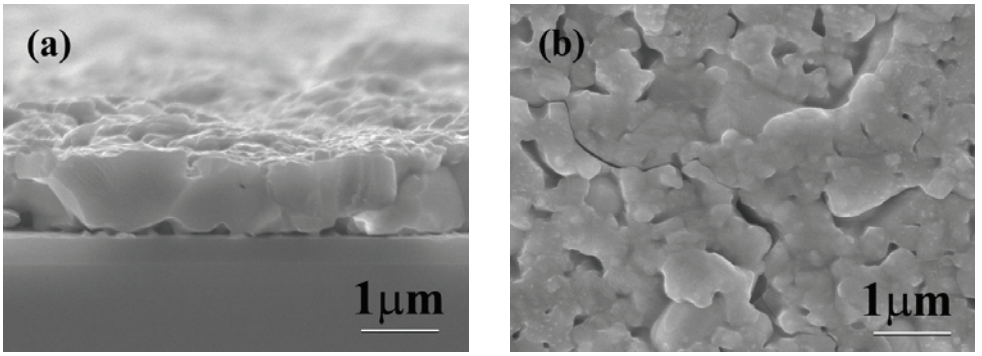

Fig. 3. SEM micrographs of as-annealed $TiFeCoNiO_y$ oxide film, (a) cross section; and (b) plan view.

We found that the copper element preferred to segregate to the surface and formed Cu-rich oxide particles in the alloys with Cu-addition. Figure 4(a) and 4(b) show cross-section and plan-view micrographs of the $Al_{0.5}CrFeCoNiCuO_y$ oxide film after annealed. This indicated that the solubility of copper atoms was not as well as the other elements; adding Cu atoms would induce the precipitation of Cu-rich oxide phase. However, the SiO_2 layer still existed after annealed, and therefore, the Si substrate had no influence on the resistivity of these thin oxide films. All of these metal oxide thin films had nanoscale FCC structures after annealed. However, they had different types and lattice constants under the as-annealed states by TEM observation.

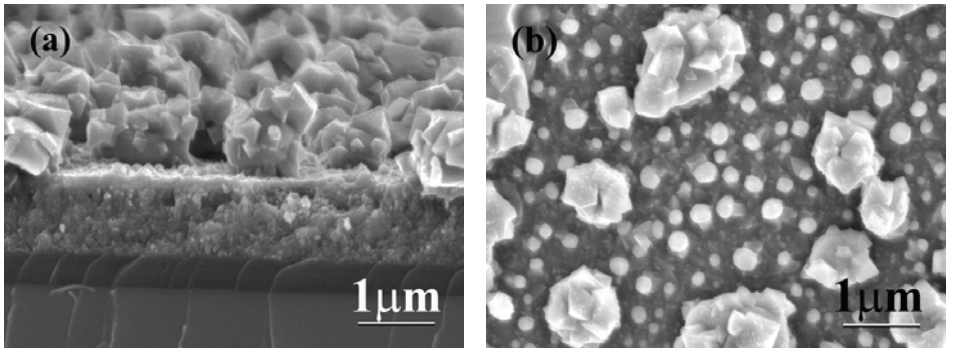

Fig. 4. SEM micrographs of as-annealed $Al_{0.5}CrFeCoNiCuO_y$ oxide film, (a) cross section; and (b) plan view.

3.3. Electrical resistivity

Figure 5 shows the room-temperature electrical resistivity of the as-annealed $TiFeCoNiO_y$ oxide films that were annealed at 1000 °C for different periods, indicating that these films had very low resistivity levels after they were annealed at 1000 °C at initial annealing stage, and had the lowest resistivity after they were annealed for about 30 min. Additionally, their resistivity increases only slightly as the annealing time increases to about 4 hr. The resistivity of these oxide thin films increased significantly after annealed for 4 hr. Figure 5 indicates that the reducing the Ti-contain would drop the lowest resistivity of the $Ti_xFeCoNiO_y$ thin films, but also decrease the oxidation resistance. That is, the

$FeCoNiO_y$ thin film had the lowest resistivity among these alloy oxide film; its resistivity increased sharply and hard to measure while annealing time was more than 4 hr. Although the lowest resistivities of these alloy oxide films are still higher than that of many pure metals, these films have extremely low resistivities among ceramic semiconductors at room temperature. This result is extremely important.

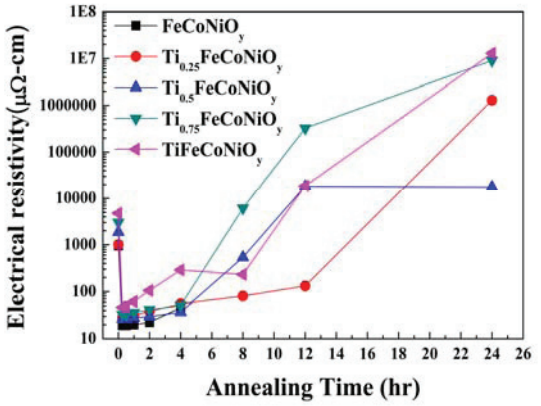

Fig. 5. Plot of the electrical resistivity of $Ti_XFeCoNiO_y$ thin films under annealing temperature of 1000 °C against annealing time.

Figure 6 shows the room-temperature electrical resistivity of the as-annealed $TiFeCoNiCu_xO_y$ oxide films that were annealed at 400 °C for different periods. The $TiFeCoNiCu_xO_y$ oxide films were annealed at the temperature range of 200-500 °C to test their resistivity. The $TiFeCoNiCu_xO_y$ oxide films were failure if the annealing temperatures were higher than 500 °C. The best annealing temperature was tested to be 400 °C. Figure 6 indicates the lowest resistivity of $TiFeCoNiCu_3O_y$ oxide film was obtained after it is annealed at 400 °C for about 4 hr. The $TiFeCoNiCuO_y$ oxide film has the lowest resistivity of about 200 μΩ-cm after vacuum annealed at 400 °C for about 3 hr. After that, the resistivity of $TiFeCoNiCu_3O_y$ oxide film increases slightly, but the resistivity of $TiFeCoNiCuO_y$ oxide film increases sharply. However, both of their resistivities are higher than that of $TixFeCoNiO_y$ films. Therefore, addition of copper has no benefit on the decreasing the resistivity of $TiFeCoNiO_v$ thin films.

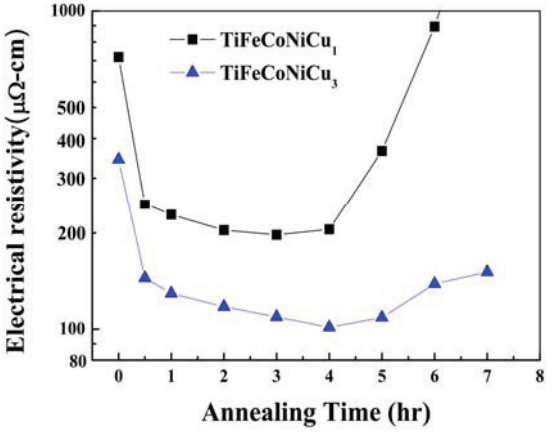

Fig. 6. Plot of the electrical resistivity of $TiFeCoNiCu_xO_y$ thin films under annealing temperature of 400 °C against annealing time.

Figure 7 shows the room-temperature electrical resistivity of the as-annealed $Al_{0.5}CrFeCoNiCuO_y$ oxide films that were annealed at different temperatures. The room-temperature electrical resistivity of the as-annealed $AlCrFeCoNiCuO_y$ oxide films did not drop significantly after annealing, and its data is not shown here. The $Al_{0.5}CrFeCoNiCuO_y$ oxide films were failure if the annealing temperatures were higher than 700 °C. The best annealing condition of $Al_{0.5}CrFeCoNiCuO_y$ oxide films is 600 °C and 15 min, the resistivity of this alloy under this condition is 550 μΩ-cm; but this thin film also has another annealing condition of 500 °C for 4 hr to get a low resistivity of 580 μΩ-cm.

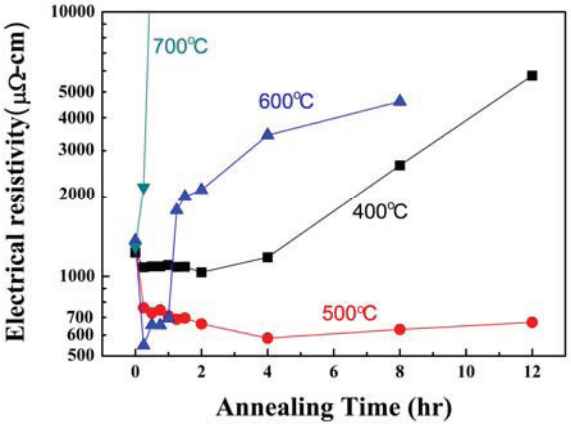

Fig. 7. Plot of the electrical resistivity of $Al_{0.5}CrFeCoNiCuOy$ thin films under different annealing temperatures against annealing time.

Table 2 lists the lowest electrical resistivity of each oxide thin film and their corresponding annealing condition. We tested the electrical resistivity of the alloy oxide thin films investigated under different annealing conditions, such as different temperatures and different times. These oxide thin films also exhibited different results. Therefore, the suitable annealing temperatures were 900~1000°C for producing $Ti_xFeCoNiO_y$ oxide films; 500~600°C for producing $Al_xCrFeCoNiCuO_y$ oxide films; and around 400°C for producing $TiFeCoNiCu_xO_y$ oxide films.

Table 2. The lowest resistivity of each oxide thin film and the corresponding annealing condition.

Alloy oxide films	Resistivity (μΩ-cm)	Vacuum annealing condition
$Al_{0.5}CrFeCoNiCuO_y$	550	600°C-15min
$AlCrFeCoNiCuO_y$	1500	500°C-15min
$FeCoNiO_y$	19	1000°C-30min
$Ti_{0.25}FeCoNiO_y$	28	1000°C-15min
$Ti_{0.5}FeCoNiO_y$	26	1000°C-15min
$Ti_{0.75}FeCoNiO_y$	31	900°C-30min
$TiFeCoNiO_y$	35	1000°C-30min
$TiFeCoNiCuO_y$	130	450°C-4hr
$TiFeCoNiCu_2O_y$	250	350°C-1hr
$TiFeCoNiCu_3O_y$	101	400°C-4hr

4. Conclusions

We used the equimolar concept to produce high entropy alloy oxide thin films, and studied their electrical resistivity. We also found out new compositions of alloy oxide thin films which had very low electrical resistivity at room temperature. Especially, the $Ti_xFeCoNiO_y$ film had very low resistivity. This result could be very important in the field of electronic ceramics. Their room-temperature resistivity are close to that of most of the metallic alloys, and lower than that of RuO_2 single crystal, also much lower than that of ITO. This effect was contributed by the oxygen vacancies. The electrical resistivities of these alloy oxide thin films were dominated by both of the compositions and oxygen-content.

Acknowledgements

The authors are grateful to National Science Council of Taiwan, Republic of China for supporting of this research under the Contract No. NSC 100-2221-E-034-009.

References

[1] Wulff J. *Structure and Properties of Materials*, Vol.4. New York: John Wiley & Sons, Inc.; 1971.

[2] Smith WF. *Foundations of Materials Science and Engineering*. 3rd Ed. New York: MaGraw-Hill, Inc; 2004.

[3] Ryden WD, Lawson AW, Sartain CC. *Phys Rev B* 1 1970; **1**: 1494.

[4] Utsumi K, Matsunaga O, Takahata T. *Thin Solid Films* 1998; **334**: 30.

[5] Huang PK, Yeh JW, Shun TT, Chen SK, *Adv Eng Mater* 2004;**6**:74.

[6] Yeh JW, Chen SK, Gan JY, Chin TS, Shun TT, Tsau CH, Chang SY. *Adv Eng Mater* 2004; **6:299**.

[7] Yeh JW, Chen SK, Gan JY, Lin SJ, Chin TS, Shun TT, Tsau CH, Chang SY. *Metall Mater Trans A* 2004; **35A:2533**.

[8] Yang YC, Tsau CH, Yeh JW. *Scripta Mater* 2011; **64:173**.

[9] Donovan TS, Heinemann K. *Phys Rev Lett* 1971; **27:1794**.

[10] Tsukimoto S, Moriyama M, Murakami M. *Thin Solid Films* 2004:**460**:222.